# Cloud-Point Phenomena in Wormlike Micellar Systems Containing Cationic Surfactant and Salt

Srinivasa R. Raghavan, Håkan Edlund, and Eric W. Kaler*

*Center for Molecular and Engineering Thermodynamics, Department of Chemical Engineering, University of Delaware, Newark, Delaware 19716*

*Received July 23, 2001. In Final Form: November 9, 2001*

Cationic surfactants with an erucyl ($C_{22}$, monounsaturated) tail display unusual phase behavior in aqueous solution as a function of temperature and added salt concentration. Low amounts of salts with binding counterions such as sodium tosylate (NaTos) lead to highly viscoelastic wormlike micellar solutions. With further addition of salt, the viscosity decreases, and the solutions cloud on heating (i.e., exhibit lower consolute phase behavior). The cloud-point temperature and the zero-shear viscosity $\eta_0$ pass in parallel through minima as a function of NaTos concentration. Cloud-point behavior is seen over a wider range of salt concentrations in the case of sodium salicylate (NaSal), which has an even stronger binding counterion. In the case of a weakly binding salt (NaCl), phase transitions are observed only at much higher salt contents, and the phase behavior is predominantly of the upper consolute type. Light and neutron scattering data show evidence of critical concentration fluctuations near the cloud point. The phase behavior and patterns of variation of rheological properties can be attributed to micellar branching, in agreement with recent theories and cryo-TEM studies.

## Introduction

In the presence of salt, long-tailed cationic surfactants can self-assemble in aqueous solution into long, flexible wormlike micelles, thus rendering the solution viscoelastic.[1,2] Salts with hydrophobic counterions, such as sodium salicylate (NaSal) and sodium tosylate (NaTos), are particularly effective in inducing micellar growth even at low concentrations. With increasing salt content, complex variations occur in the rheological properties.[1−3] The classic examples are solutions of cetyl trimethylammonium bromide (CTAB) and NaSal,[3] for which the zero-shear viscosity $\eta_0$ goes through a maximum at low NaSal concentrations, then a minimum, and subsequently a second maximum around 1 M NaSal.

High concentrations of salt can also cause cationic surfactant solutions to separate into immiscible surfactant-rich and surfactant-poor phases.[4] This phenomenon, originally termed coacervation, has been investigated since the 1940s and was first observed for mixtures of the cationic surfactant Hyamine 1622 with salts such as potassium thiocyanate (KSCN) and potassium chloride (KCl).[5,6] The phase separation is typically of the upper consolute type, i.e., it occurs on cooling below a characteristic temperature $T_c$, which, in turn, increases with salt content.[4]

On the other hand, lower consolute behavior, i.e., phase separation on heating, is typically observed for aqueous solutions of nonionic surfactants.[7] Beyond a characteristic temperature called the "cloud point", these micellar solutions turn cloudy and demix into two liquid phases. A few cationic surfactant solutions also show cloud-point behavior.[8−12] Appell and Porte[8] found cloud points at high concentrations (>3 M) of sodium chlorate ($NaClO_3$) salt in aqueous solutions of either CTAB or cetyl pyridinium bromide (CPyBr). In a later study, Warr and co-workers[9] showed that quarternary ammonium surfactants with tributyl headgroups exhibit cloud points in binary aqueous solution. Adding salt to these surfactant solutions lowers the cloud-point temperature.[10]

The present study focuses on a series of cationic surfactant and salt solutions that show a variety of unusual phase behavior. Two cationic surfactants are studied, both with an erucyl tail (i.e., a $C_{22}$ moiety with cis unsaturation at the 13-carbon position): viz., erucyl bis(hydroxyethyl)methylammonium chloride (EHAC) and erucyl trimethylammonium chloride (ETAC). Both surfactants have quarternary ammonium headgroups, with the headgroup in EHAC being slightly larger and more hydrophilic. Previously,[13] we reported the rheological behavior of EHAC and ETAC solutions containing low concentrations of NaSal and sodium chloride (NaCl). These wormlike micellar solutions displayed a remarkably pronounced viscoelasticity. Extremely high viscosities ($\eta_0 \approx 10^4$ Pa s) (and in some cases, gellike behavior) were found at room temperature, and appreciable viscosity ($\eta_0 > 10$ Pa s) was retained up to ca. 90 °C. Here, we demonstrate a rich diversity of phase behavior in these surfactant/salt mixtures. The phase behavior is sensitive

* To whom correspondence should be addressed. E-mail: kaler@che.udel.edu. Tel.: (302) 831-3553. Fax: (302) 831-6751.

(1) Rehage, H.; Hoffmann, H. *Mol. Phys.* **1991**, 74, 933.
(2) Hoffmann, H. In *Structure and Flow in Surfactant Solutions*; Herb, C. A., Prudhomme, R., Eds.; ACS Symposium Series 578; American Chemical Society: Washington, D.C., 1994; p 2.
(3) Aswal, V. K.; Goyal, P. S.; Thiyagarajan, P. *J. Phys. Chem. B* **1998**, *102*, 2469.
(4) Vassiliades, A. E. In *Cationic Surfactants*; Jungerman, E., Ed.; Marcel Dekker: New York, 1970; p 387.
(5) Booij, H. L. In *Colloid Science*; Kruyt, H. R., Ed.; Elsevier: Amsterdam, 1949; p 681.
(6) Cohen, I.; Hiskey, C. F.; Oster, G. *J. Colloid Sci.* **1954**, *9*, 243.
(7) Degiorgio, V. In *Physics of Amphiphiles: Micelles, Vesicles, and Microemulsions*; Degiorgio, V., Corti, M., Eds.; North-Holland Publishers: Amsterdam, 1983; p 303.
(8) Appell, J.; Porte, G. *J. Phys. (Paris) Lett.* **1983**, *44*, L689.
(9) Warr, G. G.; Zemb, T. N.; Drifford, M. *J. Phys. Chem.* **1990**, *94*, 3086.
(10) Buckingham, S. A.; Garvey, C. J.; Warr, G. G. *J. Phys. Chem.* **1993**, *97*, 10236.
(11) Kubota, K.; Kuwahara, N.; Sato, H. *J. Chem. Phys.* **1994**, *100*, 4543.
(12) Martin, A.; Lopez, I.; Monroy, F.; Casielles, A. G.; Ortega, F.; Rubio, R. G. *J. Chem. Phys.* **1994**, *101*, 6874.
(13) Raghavan, S. R.; Kaler, E. W. *Langmuir* **2001**, *17*, 300.

10.1021/la011148e CCC: $22.00 
Published on Web 01/23/2002

to the specific salt, with NaCl, NaTos, and NaSal showing three different classes of behavior. The microscopic origin of these diverse phenomena is investigated using a combination of phase behavior studies, rheology, and scattering techniques.

## Experimental Section

**Materials.** EHAC and ETAC surfactants were commercial products from Akzo Nobel (Chicago, IL) and Witco Chemical Corp. (Memphis, TN), respectively. Their chemical structures are shown below

EHAC 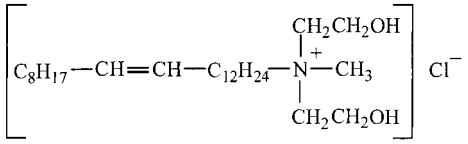

ETAC 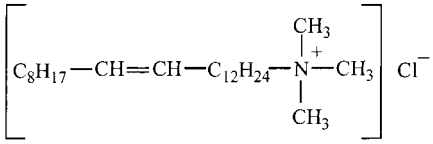

The surfactants are synthesized from erucic acid, an unsaturated fatty acid. Some polydispersity (5−10%) is expected in the hydrocarbon chain length, and about 1% of the chains might be saturated.[14] Sodium salicylate (*o*-hydroxy benzoate), sodium tosylate (*p*-toluene sulfonate), and sodium chloride were ACS-grade reagents (>99% purity) purchased from Aldrich. Solutions containing surfactant and salt were prepared using distilled deionized water.

**Phase Behavior.** Phase behavior was recorded by visual observation. The phase boundaries as a function of temperature were determined by noting the incipient formation of a second phase on heating or cooling (transitions were always determined from one-phase to two-phase states). Near the lower consolute phase boundary, the entire sample turned cloudy on heating. The transition temperatures reported here are reproducible to within ±0.5 °C. Isothermal phase behavior was recorded through observations of samples equilibrated in a water bath at 25 °C.

**Rheology.** Rheological experiments were performed on a Bohlin CS-10 stress-controlled rheometer. A couette geometry was used with a cup of 27.5 mm diameter and a bob 25 mm by 37.5 mm. The cell was heated by fluid circulating from a Neslab high-temperature bath. A cover made of temperature-resistant polymer minimized water evaporation.

**Static Light Scattering (SLS).** Samples for SLS were transferred into 2-mL ampules and held in a vat of *trans*-decalin. The temperature of the vat was controlled to within ±0.1 °C. The light source was a 300-mW argon ion laser with a wavelength $\lambda$ of 488 nm. Light scattered by the sample was collected by a photomultiplier tube mounted on the arm of a Brookhaven BI-200SM goniometer, and scattering angles between 30° and 135° were probed. Intensities are reported relative to benzene. The scattering vector $q$ is defined here as $q = (4\pi n/\lambda)\sin(\theta/2)$, where $\theta$ is the scattering angle and $n$ is the refractive index of the solution.

**Small-Angle Neutron Scattering (SANS).** The SANS experiments were performed on the NG-3 spectrometer at the Cold Neutron Research Facility of the National Institute of Standards and Technology (NIST) in Gaithersburg, MD. The incident neutron wavelength was 6 Å with a 15% spread. Quartz cells with 2-mm path lengths were used, and the samples were placed in a temperature-controlled chamber. Three different sample-to-detector distances were used to span a range of 0.004−0.4 Å$^{-1}$ in the scattering vector $q$. The scattering spectra were corrected for background radiation, detector efficiency, empty cell scattering, and sample transmission. The spectra were radially averaged and placed on an absolute scale using calibration standards provided by NIST. The data are shown in terms of the absolute scattered intensity $I$ as a function of the scattering vector $q = (4\pi/\lambda)\sin(\theta/2)$, where $\lambda$ is the wavelength of incident neutrons and $\theta$ is the scattering angle.

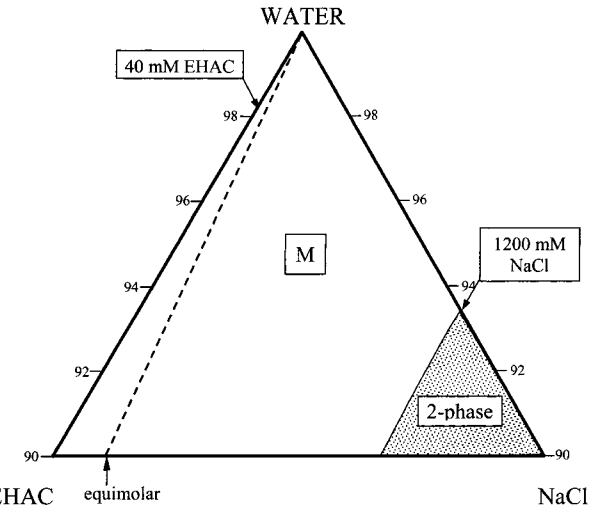


**Figure 1.** Water-rich corner of the EHAC/NaCl/water phase diagram at 25 °C. All concentrations are in weight percentages. Solutions in the one-phase region (marked M) consist of cylindrical micelles. In the two-phase region, two liquidlike phases coexist, with one containing most of the surfactant. Equivalent molar compositions are also indicated.

## Results

**A. Phase Behavior and Rheology.** *EHAC/NaCl.* We begin with the phase behavior of EHAC/NaCl mixtures at 25 °C in the water-rich corner of the EHAC/NaCl/water triangular phase diagram (Figure 1). Isotropic, one-phase solutions are found until $c_{NaCl} = 1200$ mM, beyond which the solutions demix into two isotropic liquid phases. The upper phase is bluish, viscoelastic, and flow-birefringent, whereas the lower phase is clear and nonviscous. The upper phase is thus similar to the viscoelastic solutions in the one-phase region (see below). Evidently, the surfactant is mostly confined to this upper phase, henceforth called the "coacervate", whereas the lower phase contains very little surfactant. Phase separation occurs at nearly the same value of $c_{NaCl}$ for a wide range of EHAC concentrations (1−80 mM). The volume of the coacervate phase, however, varies significantly with $c_{NaCl}$ for a given surfactant content. The coacervate occupies nearly the entire sample volume close to the phase boundary but shrinks as more salt is added. This coacervation behavior, on first glance, appears similar to that in other systems.[4,6]

The first unusual phenomena are seen in the temperature dependence of the EHAC/NaCl phase behavior. The coexistence curve is shown in Figure 2a for a constant $c_{EHAC} = 40$ mM. As with other coacervating systems,[4,6] the EHAC/NaCl system shows the upper consolute type of phase behavior, i.e., the solutions phase separate on cooling below the coexistence temperature $T^*$. Whereas previous studies found a linear increase in $T^*$ with salt, however, $T^*$ here varies little at low $c_{NaCl}$ and increases steeply around 1200 mM NaCl. For $c_{NaCl} > 1200$ mM, the samples are biphasic at all temperatures. Furthermore, in the concentration range 1100−1200 mM NaCl, the phase behavior is anomalous and erratic. The solutions become cloudy when heated to ca. 40 °C, but clear at higher temperatures. This suggests that there is a small miscibility loop in this region of the phase diagram. However,

(14) Lin, Z.; Chou, L. C.; Lu, B.; Davis, H. T.; Scriven, L. E.; Talmon, Y.; Zakin, J. L. *Rheol. Acta* **2000**, *39*, 354.

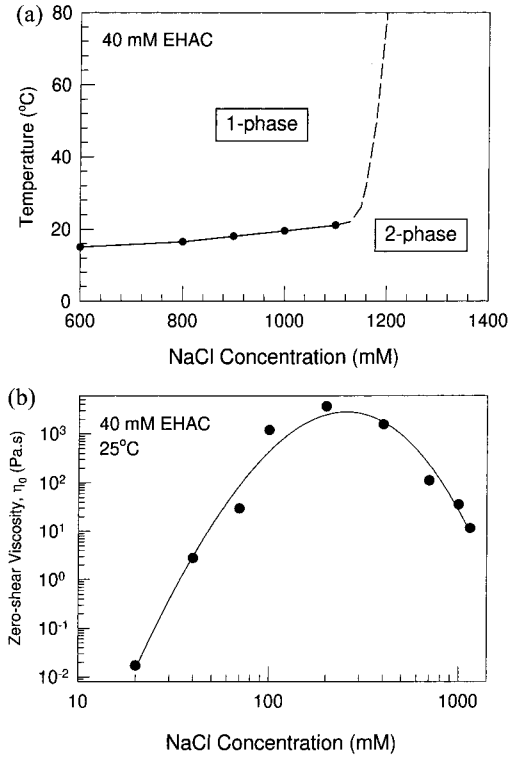


**Figure 2.** Phase behavior and rheology as a function of $c_{NaCl}$ for a fixed EHAC content of 40 mM. (a) Coexistence temperature and (b) zero-shear viscosity $\eta_0$ at 25 °C.

this behavior cannot be reproduced satisfactorily, and so only a dashed line is shown in Figure 2a for this composition range. Interestingly, Appell and Porte[8] also observed such erratic behavior as a function of temperature for CPyBr/$NaClO_3$ mixtures at very high salt concentrations (>3 M).

The zero-shear viscosity $\eta_0$ of EHAC/NaCl solutions at 25 °C is shown as a function of salt for a fixed $c_{EHAC}$ of 40 mM (Figure 2b). The viscosity increases to a maximum at ca. 200 mM NaCl and decreases thereafter. Samples in the vicinity of the maximum are in fact *gels*—so-called because, in those cases, the viscosity continues to rise at low shear-rates instead of showing a Newtonian plateau. A gellike response is also observed for other EHAC/salt systems and has been discussed in detail elsewhere.[13] The indicated values of $\eta_0$ for the gellike samples in Figure 2b correspond to the viscosity at the lowest measurable shear rate ($\sim 10^{-4}$ $s^{-1}$). Note that the zero-shear viscosity $\eta_0$ drops steadily until the point of phase separation.

*EHAC/NaTos.* Next, we consider the phase behavior of EHAC/NaTos mixtures at 25 °C. In contrast to $Cl^-$, $Tos^-$ is hydrophobic and can penetrate between the surfactant headgroups on a micelle and into the hydrophobic interior. The triangular phase diagram for EHAC/NaTos/water at 25 °C (Figure 3) shows a closed biphasic region at intermediate compositions. A line of constant $c_{EHAC}$ can cut the two-phase body at two points. For example, adding NaTos to 40 mM EHAC solutions initially causes a transition from one to two phases at 90 mM NaTos, and further salt addition allows a single phase to form at 150 mM NaTos. Samples with high surfactant loadings ($c_{EHAC}$ > 90 mM), on the other hand, are monophasic over the entire range of compositions.

Coexistence temperatures as a function of $c_{NaTos}$ are shown for two different EHAC concentrations of 40 and 100 mM (Figure 4a). The EHAC/NaTos solutions turn cloudy on heating, indicative of lower consolute phase

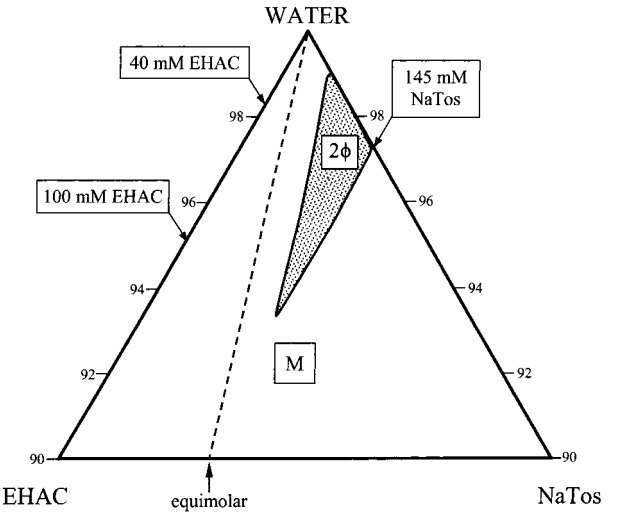


**Figure 3.** Water-rich corner of the EHAC/NaTos/water phase diagram (in wt %) at 25 °C. The one-phase region marked M consists of cylindrical micelles. In the two-phase region, two liquid phases coexist. Equivalent molar compositions are also shown in the figure.

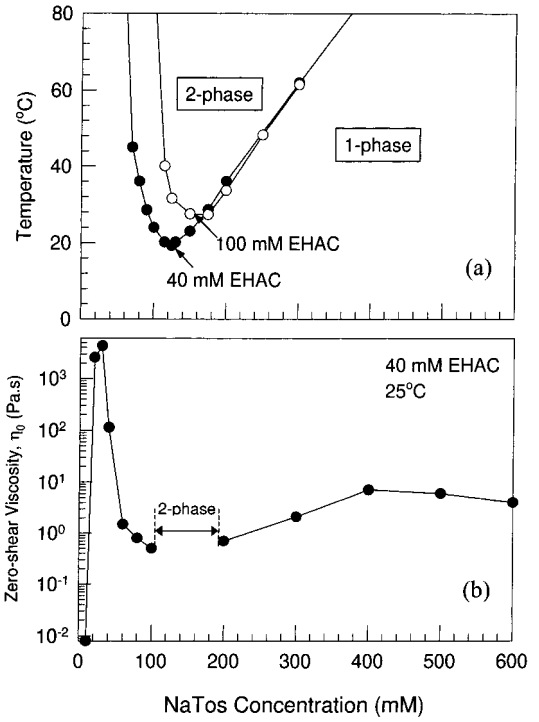


**Figure 4.** Phase behavior and rheology as a function of NaTos concentration. (a) Coexistence temperature vs $c_{NaTos}$ for $c_{EHAC}$ = 40 and 100 mM. (b) Zero-shear viscosity $\eta_0$ at 25 °C vs $c_{NaTos}$ for 40 mM EHAC.

behavior. The coexistence (cloud-point) temperature passes through a minimum as a function of $c_{NaTos}$. Increasing $c_{EHAC}$ from 40 to 100 mM shifts the left branch of the curve to slightly higher salt concentrations but does not alter the portion of the curve at higher salt content.

The zero-shear viscosity $\eta_0$ at 25 °C for 40 mM EHAC solutions shows two maxima as a function of $c_{NaTos}$ (Figure 4b). The first viscosity maximum occurs at low salt content ($\sim$20 mM), and the corresponding samples are gellike. Note that the penetrating $Tos^-$ counterions induce micellar growth at very low concentrations. Beyond the viscosity maximum, further addition of NaTos causes a precipitous drop in viscosity, followed eventually by phase separation. A comparison of the graphs in Figure 4a and b shows that

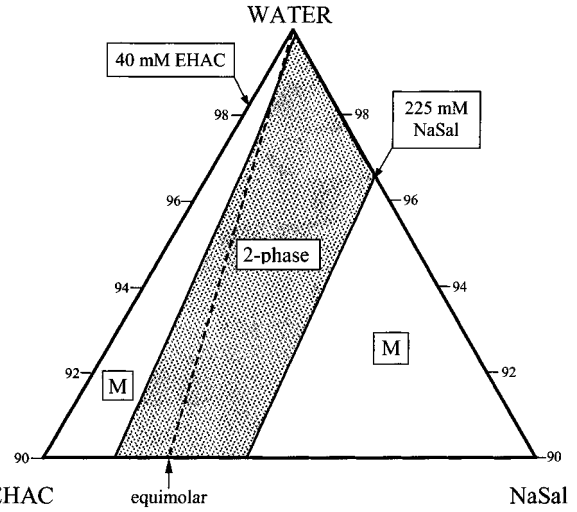


**Figure 5.** Water-rich corner of the EHAC/NaSal/water phase diagram (in wt %) at 25 °C. Samples in the one-phase regions marked M contain cylindrical micelles, whereas those in the two-phase region separate into two liquid phases. Equivalent molar compositions are also indicated.

the viscosity and cloud-point curve both pass through minima around the same salt concentration. At much higher $c_{NaTos}$ (∼400 mM), a second and milder maximum is found in the viscosity.

*EHAC/NaSal.* We now consider the phase behavior of EHAC/NaSal mixtures at 25 °C. The $Sal^-$ counterion is also hydrophobic and can bind to micelles. The triangular phase diagram for EHAC/NaSal/water at 25 °C (Figure 5) shows a biphasic region over a large composition range. For each $c_{EHAC}$, there are two intersection points with the two-phase body. At 40 mM EHAC, for example, adding just 32 mM NaSal induces demixing, and the single phase reappears at 240 mM NaSal. Note that the boundaries of the two-phase body are roughly parallel. As $c_{EHAC}$ is increased, slightly larger NaSal concentrations are required both to enter and to exit the two-phase region.

Coexistence temperatures as a function of $c_{NaSal}$ are shown for a $c_{EHAC}$ of 40 mM in Figure 6a. Upon addition of 32 mM NaSal, the samples phase separate at ambient temperature; however, these samples revert to a single phase on heating. Such upper consolute phase behavior is observed over a narrow range of salt concentrations. Further salt addition renders the samples biphasic over all temperatures. Subsequently, at around 150 mM NaSal, the samples become monophasic at low temperatures but turn cloudy on heating to the coexistence temperature. This corresponds to lower consolute phase behavior and is seen for all higher salt concentrations. With increasing $c_{NaSal}$, the coexistence (cloud-point) temperature monotonically increases (Figure 6a).

The phase volumes in the two-phase region were studied as a function of the salt content (Figure 6b). For these studies, samples were placed in graduated tubes at 25 °C to monitor the phase volumes (steady state was reached within 1 week). Each sample separated into a surfactant-rich coacervate phase (with a bluish or light-greyish tinge) and a clear solution. Various compositions are illustrated schematically in Figure 6b, with the gray region representing the coacervate. At the onset of phase separation (32 mM NaSal), the coacervate is of low density and occupies nearly the entire sample volume. As the NaSal content increases, the coacervate volume shrinks significantly, and the denser coacervate sinks to the bottom of the container. The maximum density is reached at the middle of the two-phase region. Beyond ca. 150 mM NaSal,

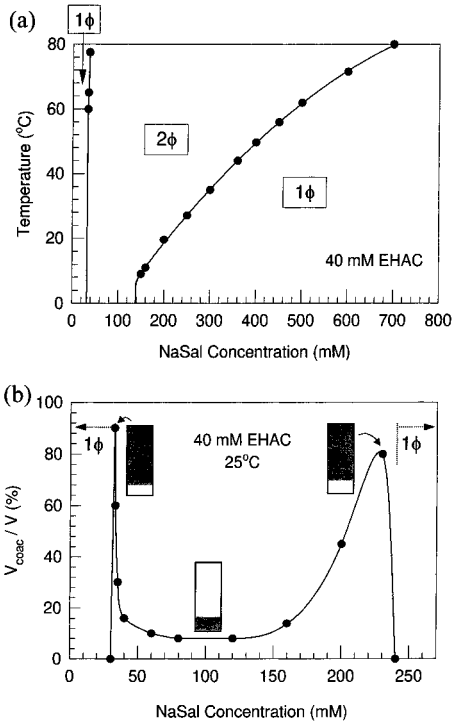


**Figure 6.** Phase behavior as a function of $c_{NaSal}$ for a fixed EHAC content of 40 mM. (a) Coexistence temperature $T_c$ vs $c_{NaSal}$. (b) Relative volume of the coacervate layer (at 25 °C) in the two-phase samples as a function of $c_{NaSal}$. The sample separates into a surfactant-rich coacervate (shaded gray) and a salt solution (unshaded). At the onset of phase separation (∼32 mM NaSal), the coacervate is of low density and occupies nearly the entire sample volume. With increasing salt concentration, the coacervate becomes more dense and settles to the bottom of the vial. The coacervate phase swells with a further increase in salt content and again fills the sample until a single phase is eventually recovered at ∼240 mM salt.

the density decreases again, and the coacervate fills a larger fraction of the volume. Eventually, the lighter coacervate rises to the top of the container, and just before the second single-phase region, the coacervate again fills nearly the entire volume.

With the phase behavior in hand, the rheology of EHAC/NaSal solutions can be addressed sensibly as a function of both salt and surfactant concentration. The zero-shear viscosity $\eta_0$ at 25 °C as a function of $c_{NaSal}$ describes two maxima (Figure 7a), similarly to the viscosity data as a function of $c_{NaTos}$. The first viscosity maximum again occurs at low $c_{NaSal}$ (∼20 mM), and the corresponding samples are gellike. (The rheology at low $c_{NaSal}$ is discussed in detail elsewhere.[13]) Further salt addition causes a steep drop in viscosity, then a wide two-phase region, and finally a second viscosity maximum around 600 mM NaSal. Varying the surfactant concentration at a fixed value of $c_{NaSal}$ (450 mM) causes $\eta_0$ to increase and then level off at higher surfactant loadings (Figure 7b). The plateau modulus $G_p$ increases steadily with $c_{EHAC}$ according to the relation $G_p \approx (c_{EHAC})^{2.1}$. The observed power-law exponent in the range 2.0−2.2 is characteristic of wormlike micelles.[2]

The temperature dependence of rheological parameters was investigated for a sample showing cloud-point behavior, viz., 40 mM EHAC + 450 mM NaSal, which phase separates at 53 °C. Steady and dynamic rheological experiments were conducted between 20 and 52 °C on this sample. At all temperatures, the dynamic response (Figure 8a) is that of a Maxwell fluid with a single relaxation time, which is a signature of wormlike micelles. The elastic ($G'$) and viscous ($G''$) moduli of a Maxwell fluid

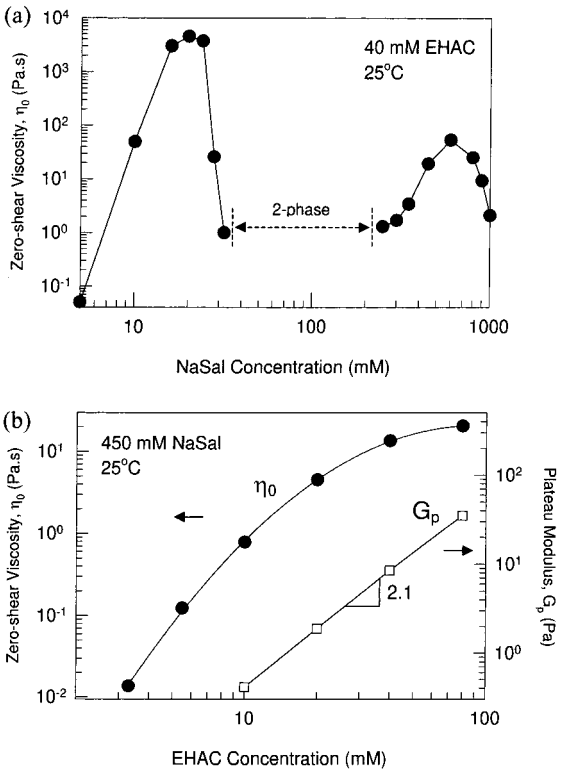


**Figure 7.** Rheology of EHAC/NaSal solutions at 25 °C. (a) Zero-shear viscosity $\eta_0$ vs $c_{NaSal}$ for 40 mM EHAC. (b) Zero-shear viscosity $\eta_0$ and plateau modulus $G_p$ vs $c_{EHAC}$ for 450 mM NaSal.

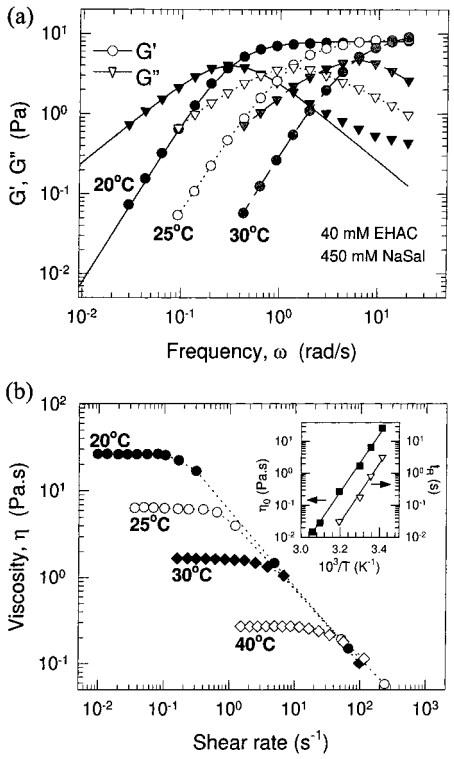


**Figure 8.** Rheology at various temperatures for a solution of 40 mM EHAC and 450 mM NaSal. (a) Dynamic rheology and (b) steady-shear rheology. The solid lines in a through the data at 20 °C are fits to the Maxwell model (eqs 1 and 2). The inset in b is an Arrhenius plot of the zero-shear viscosity $\eta_0$ and relaxation time $t_R$ vs $1/T$. The slopes of the two straight lines are identical and yield the activation energy $E_a$ (eqs 3 and 4).

are described by[2]

$$G'(\omega) = \frac{G_p \omega^2 {t_R}^2}{1 + \omega^2 {t_R}^2} \quad (1)$$

$$G''(\omega) = \frac{G_p \omega t_R}{1 + \omega^2 {t_R}^2} \quad (2)$$

Fits of eqs 1 and 2 to the data at 20 °C are included as solid lines in Figure 8a. The data depart from the Maxwellian response only at high frequencies where an upturn in $G''$ occurs as a result of the appearance of "breathing" or Rouse relaxation modes.[4] With increasing temperature, the entire frequency spectrum shifts to higher frequencies (i.e., shorter time scales), with the plateau modulus $G_p$ remaining constant. The relaxation time $t_R$, given by the inverse of the frequency at which $G'$ and $G''$ intersect, decreases rapidly on heating. Beyond 30 °C, $t_R$ is very low, and the weak dynamic response is not shown.

Under steady shear (Figure 8b), a low-shear viscosity plateau is observed at all temperatures, with $\eta_0$ satisfying the Maxwell fluid relation ($\eta_0 = G_p t_R$). As temperature is increased, there is a progressive drop in $\eta_0$. An Arrhenius plot of $\eta_0$ and $t_R$ vs $1/T$, where $T$ is the absolute temperature (Figure 8b, inset), shows the expected exponential decrease in these quantities with temperature, as given by the following relations[13]

$$t_R = A e^{E_a/RT} \quad (3)$$

$$\eta_0 = G_p A e^{E_a/RT} \quad (4)$$

Here, $E_a$ is the flow activation energy, $R$ is the gas constant, and $A$ is a preexponential factor. The straight-line fits through the $t_R$ and $\eta_0$ data have the same slope (because $G_p$ is independent of temperature) and yield a value for the activation energy $E_a$ of 198 kJ/mol. The significant point to be drawn from Figure 8 is that the rheology is no different from that of typical wormlike micellar systems even though the sample displays a cloud point. The viscosity shows a steady exponential decrease with temperature until the onset of phase separation. The viscosity does fall to a low value (~0.01 Pa s) prior to phase separation.

*EHAC/NaSal + NaCl.* NaSal/NaCl mixtures were examined to learn how mixtures of binding and nonbinding counterions influence the phase behavior of EHAC. The NaCl concentration was fixed at 400 mM, and the EHAC concentration at 40 mM. At this composition, an EHAC/NaCl solution is a single phase at all temperatures. However, adding even a small amount of NaSal to this solution causes the sample to demix and remain biphasic over the entire range of temperatures (Figure 9). At higher NaSal contents, a single phase reappears, and the samples cloud on heating. The corresponding cloud-point temperatures are essentially the same as those for samples with no NaCl. Thus, the additional electrostatic screening introduced by the nonbinding $Cl^-$ counterions destabilizes the low-$c_{NaSal}$ samples but has no effect on the high-$c_{NaSal}$ samples.

*ETAC/NaSal.* The EHAC headgroup contains two hydroxyethyl moieties, and the question is whether this large headgroup is responsible for the unusual phase behavior of EHAC. To examine this issue, we studied the ETAC surfactant, which contains a conventional trimethylammonium headgroup and the same erucyl ($C_{22}$) chain. Remarkably, the two surfactants exhibit almost identical phase behavior with NaSal, at least for a

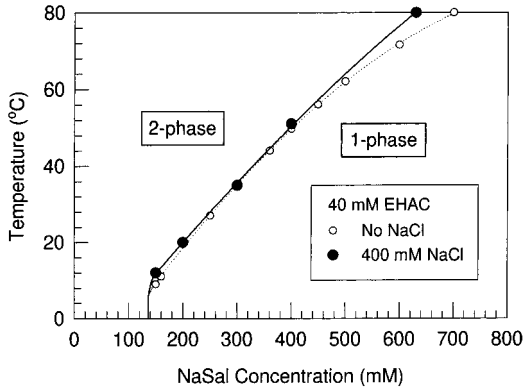


**Figure 9.** Phase behavior of EHAC and NaSal in the presence of 400 mM NaCl. The coexistence temperature is plotted vs $c_{NaSal}$ for 40 mM EHAC. In the presence of NaCl, there is no one-phase region at low NaSal content, and the coexistence temperatures at high NaSal are practically unchanged.

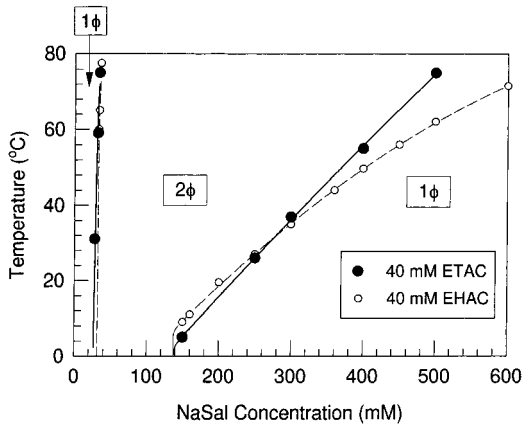


**Figure 10.** Effect of surfactant headgroup structure on the phase behavior with NaSal. The surfactants being compared have identical tails and different headgroups, viz., trimethylammonium (ETAC) and bis(hydroxyethyl)methylammonium (EHAC). The data show the coexistence temperature vs $c_{NaSal}$ for 40 mM surfactant solutions.

surfactant concentration of 40 mM (Figure 10). The coexistence temperatures for EHAC and ETAC are nearly equal for a given composition (only at high NaSal is there a slight mismatch). Thus, surprisingly, the headgroup is rather inconsequential to the phase behavior; instead, it is the long unsaturated tailgroup that seems to drive these phenomena.

**B. Light and Neutron Scattering.** The microstructures of EHAC/NaSal solutions in the one-phase region were examined by small-angle neutron scattering (SANS). These experiments were performed on 60 mM EHAC solutions in $D_2O$ containing various amounts of NaSal. Although the phase boundaries in $D_2O$ are slightly shifted compared to those in $H_2O$, the qualitative features of the phase behavior are identical.

Consider first the low-NaSal samples, for which SANS spectra are shown at 25 °C (Figure 11a). The scattered intensities $I$ are identical at high $q$ for the three samples. At low $q$, on the other hand, $I$ increases progressively with salt content. For the 18 and 30 mM NaSal solutions, $I$ describes a plateau at low $q$, whereas for 36 mM NaSal, $I$ increases with decreasing $q$. On the basis of observations of viscoelasticity and flow birefringence, these EHAC/NaSal solutions are expected to contain long, flexible cylindrical micelles.[13] The SANS spectra, however, do not show the signature of such long micelles, viz., a region at intermediate $q$ where $I \sim q^{-1}$. Moreover, the 18 and 30

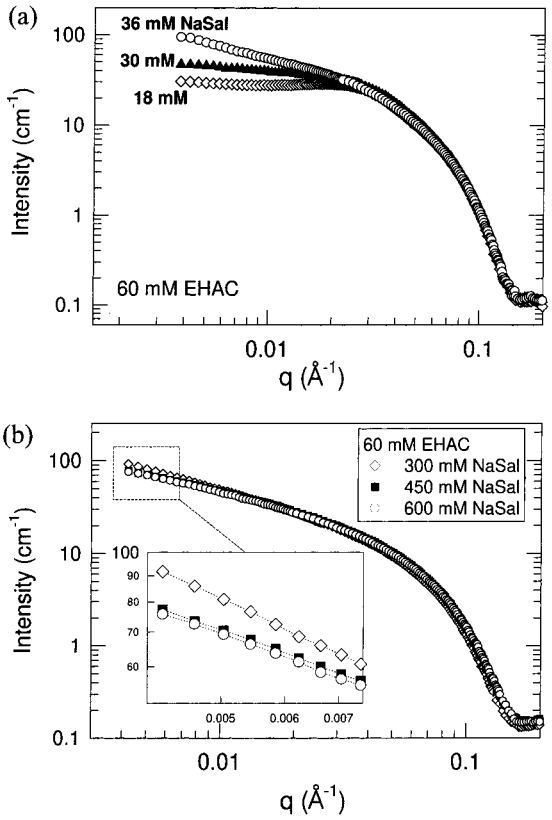


**Figure 11.** SANS spectra at 25 °C for solutions in $D_2O$ containing a fixed EHAC concentration of 60 mM and various NaSal contents. (a) $c_{NaSal} = 18$, 30, and 36 mM. (b) $c_{NaSal} = 300$, 450, and 600 mM. The inset in b is an enlargement of the low-$q$ data.

mM NaSal samples are gellike ($\eta_0 > 10^3$ Pa s), whereas the 36 mM NaSal sample has a low viscosity ($\eta_0 \approx 0.1$ Pa s). SANS, on the other hand, shows a monotonic trend with salt. Thus, there is no obvious correlation between the structure on length scales probed by SANS and the rheology.

The $q^{-1}$ region could be obscured by the influence of unscreened electrostatic interactions on the low-$q$ scattering.[15] However, the binding of salicylate counterions should substantially screen the charge on EHAC micelles even at low $c_{NaSal}$, and there is no interaction peak in the SANS spectra. Instead, it is the presence of a phase boundary nearby in composition space that seems to dictate the SANS scattering. For 60 mM EHAC solutions in $D_2O$, an upper consolute boundary begins around 38 mM NaSal, and the 36 mM NaSal sample, which exhibits the highest scattering intensity at low $q$, is the one closest to this phase boundary.

SANS spectra at 25 °C are shown in Figure 11b for high-NaSal samples that cloud on heating. The three spectra shown are practically identical except for slight differences in the scattered intensity at low $q$ (see inset). The 300 mM NaSal sample, which has the lowest cloud-point temperature $T^*$ among the three (28 °C), is the closest to a phase boundary at 25 °C and scatters most strongly. The samples with 450 and 600 mM NaSal ($T^* = 58$ and 77 °C, respectively) show nearly the same spectra. The 450 mM NaSal sample was also probed as a function of temperature by SANS (Figure 12). The spectra are again indistinguishable at high $q$, but at low $q$, the scattering increases with temperature as the sample approaches its

(15) Koehler, R. D.; Raghavan, S. R.; Kaler, E. W. *J. Phys. Chem. B* **2000**, *104*, 11035.

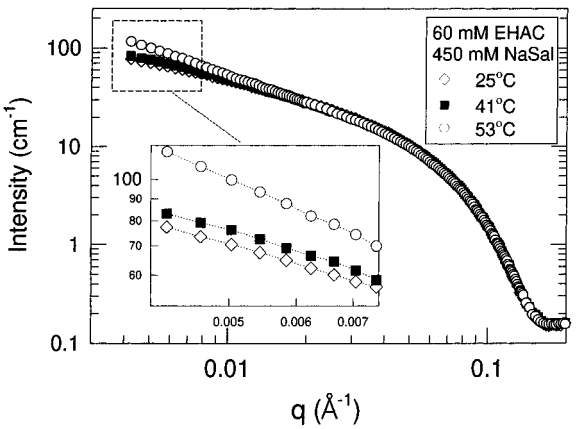


**Figure 12.** SANS spectra at various temperatures for a solution of 60 mM EHAC and 450 mM NaSal in $D_2O$. This sample phase separates above 58 °C. The inset is an enlargement of the low-$q$ data and clearly shows the increase in scattered intensity as the phase boundary is approached.

cloud point ($T^* = 58$ °C). Note that the viscosity decreases exponentially with temperature (Figure 8), suggesting that the mean micellar size decreases upon heating.[13] The increase in SANS intensity with temperature hence *cannot* be attributed to the formation of larger structures in solution.

The correlation between the scattered intensity at low $q$ and the proximity of the phase boundary suggests that the scattering increase is due to critical concentration fluctuations. In that case, the scattering should follow the Ornstein−Zernike relation[16]

$$I(q) = \frac{I_0}{1 + q^2\xi^2} \tag{5}$$

Here, $I_0$ is the intensity in the limit of $q \to 0$ and $\xi$ is the correlation length of the concentration fluctuations. As the critical temperature $T_c$ is approached, the sample is expected to scatter more intensely, with the correlation length $\xi$ diverging according to a power law in the reduced temperature $\epsilon = |T - T_c|/T_c$[16]

$$\xi = \xi_0\epsilon^{-\nu} \tag{6}$$

Static light scattering (SLS) was used to probe critical effects in an EHAC/NaSal sample that clouds on heating, viz., 40 mM EHAC + 450 mM NaSal in $H_2O$, for which the rheology was earlier shown as a function of temperature in Figure 8. This sample is an off-critical composition in the broad vicinity of a critical line. As expected, the sample scatters more strongly as it approaches its cloud point ($T^* = 53$ °C), and plots of $1/I$ vs $q^2$ at 25, 45, and 52 °C (Figure 13a) are straight lines. The Ornstein−Zernike correlation length $\xi$ extracted from the data is plotted against the reduced temperature $\epsilon$ (defined in terms of $T^*$) in Figure 13b. The data are fitted in the vicinity of $T^*$ by eq 6 with $\nu = 0.15$ and $\xi_0 = 135$ Å.

## Discussion

**Analysis of Scattering Data.** The increase in scattered light intensity on heating, the validity of the Ornstein−Zernike relation, and the power law in the correlation length all point to critical behavior. Renormalization group

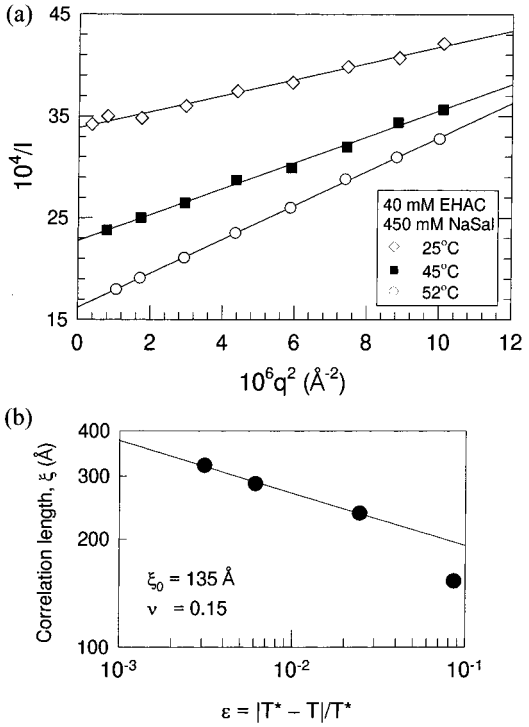


**Figure 13.** Static light-scattering data as a function of temperature for an aqueous solution containing of 40 mM EHAC and 450 mM NaSal. (a) Plots of $1/I$ vs $q^2$, where $I$ is the scattered intensity and $q$ is the wave vector (Ornstein−Zernike plots), at three different temperatures. The sample shows a cloud point $T^*$ at 53 °C. (b) Correlation length $\xi$ as a function of the reduced temperature $\epsilon$. The data are fitted to a power law (eq 6) to obtain the parameters $\xi_0$ and $\nu$.

theory predicts $\nu = 0.63$ for a binary critical point.[16] The off-critical EHAC/NaSal sample instead gives $\nu = 0.15$, implying a weak divergence of the length scale $\xi$ of these critical fluctuations. A similarly low value of $\nu$ was also found by Yu and Neuman[17] for a mixture of 25 mM sodium perfluoro octanoate and 190 mM tetrapropylammonium bromide, which also clouded on heating but was far from a critical point. The rather high value of 135 Å for the prefactor $\xi_0$ is consistent with the presence of large micellar objects in the EHAC/NaSal solution, as indicated also by the solution rheology. A large $\xi_0$ (~200 Å) was also reported for wormlike micellar solutions of CPyBr/$NaClO_3$ (these solutions gave a $\nu \approx 0.6$).[8] In contrast, $\xi_0$ values for critical microemulsions and nonionic surfactant solutions are less than 10 Å.[7,16]

The SANS data reflect a combination of critical effects and scattering from the micelles themselves. The Ornstein−Zernike expression alone cannot account for the SANS data over the entire $q$ range, but because the critical fluctuations have correlation lengths of ~200 Å, their effect is predominant at low $q$ (this is probably why the $q^{-1}$ region is absent.) The upturn in low-$q$ scattering near the cloud point can also be interpreted in terms of attractive intermicellar interactions, as demonstrated previously for nonionic surfactant solutions.[7,19] At high $q$, the dominant contribution to the scattering is from the micellar cross section. A Guinier-like plot [i.e., $\ln(Iq)$ vs $q^2$] of the high-$q$ data yields a cross-sectional radius of 29 Å for the EHAC

(16) Candau, S. J. In *Surfactant Solutions: New Methods of Investigation*; Zana, R., Ed.; Surfactant Science Series No. 22; Marcel Dekker: New York, 1987; p 147.

(17) Yu, Z.-J.; Neuman, R. D. *Langmuir* **1994**, *10*, 377.

(18) Cates, M. E.; Candau, S. J. *J. Phys. Condens. Matter* **1990**, *2*, 6869.

(19) Hayter, J. B. In *Physics of Amphiphiles: Micelles, Vesicles, and Microemulsions*; Degiorgio, V., Corti, M., Eds.; North-Holland Publishers: Amsterdam, 1983; p 59.

micelles, which is close to the length of a fully extended, monounsaturated $C_{22}$ chain (ca. 33 Å).

**Mechanisms for Phase Separation.** We have shown that EHAC/salt solutions phase separate upon either heating or cooling depending on the salt type and composition. Phase separation on *cooling* is akin to a gas−liquid transition[20] and occurs when attractive interactions between the constituent entities become sizable with respect to the thermal energy $k_BT$. In the present case, adding salt screens the electrostatic repulsions between the EHAC micelles. An attractive potential well due to van der Waals forces can then arise between the micelles, eventually causing phase separation at low temperatures.[4] Adding more salt weakens repulsions, and the system therefore phase separates at higher temperatures.

Phase separation on *heating* is a more complex phenomenon and has been explored in detail previously in the context of nonionic surfactant phase behavior. In the few cases where this phenomenon has been observed for ionic surfactant solutions, the surfactant headgroup was large and hydrophobic[9,10] or the salt concentrations were extremely high.[8] The results here show that neither of these factors is the key requirement. A comparison of EHAC and ETAC (Figures 6 and 7) shows that the headgroup is unimportant, and even low amounts of salt (e.g., less than 60 mM NaTos) are sufficient to cause these re-entrant phase transitions (Figure 5). What, then, controls the phase separation on heating? Two different arguments are presented below.

*(a) Attractive Interactions Between Pseudo-Nonionic Micelles.* One possibility is that EHAC behaves as a nonionic molecule in the presence of strongly binding salt counterions. The phase separation on heating would then be a natural outcome of the nonionic micellar character. This stems from the observation that clouding occurs only in the presence of hydrophobic counterions such as salicylate and tosylate that remain strongly bound to micelles[1,21−23] (the bound fraction of salicylate was estimated at 93% by self-diffusion studies[21]). These counterions are supposed to be oriented perpendicular to the micellar surface plane, with the hydrophobic portion penetrating into the nonpolar interior of the micelles and the negative charge located at the surface adjacent to the positively charged surfactant headgroups.[22] The headgroups and the counterions can thus form complexes at the micellar surface, and the neutralization of surface charge imparts nonionic character to the micelles. Interestingly, such pseudo-nonionic complexes have been found in some mixtures of cationic and anionic surfactants[17,24−27] (e.g., tetrapropylammonium bromide + sodium perfluoro octanoate), and indeed these mixtures show cloud points.

The nonionic character of the micelles will then be a function of composition and will depend especially on the fraction of salt that remains bound to the micelles. In the case of NaTos, the minimum in the EHAC/NaTos cloud-point curve likely corresponds to saturation binding. At this point, the micelles would be predominantly "nonionic", giving the lowest cloud-point temperature. Adding more NaTos causes a further (weak) adsorptive binding of tosylate ions at the micellar surface. This would impart a small negative charge to the micelles, which would shift the cloud-point temperature upward (in the same way that small amounts of ionic cosurfactant shift the cloud point of nonionic surfactant solutions upward[7]).

The discussion thus far assumes that pseudo-nonionic micelles will develop attractive interactions on heating. The molecular origin of such attractions is a matter of speculation, and it is not evident that hydrogen-bonding interactions play a role. Warr et al.[9,10] advanced a mechanism involving hydration shells to account for cloud points, whereas Appell and Porte[8] interpreted the clouding of CPyBr/$NaClO_3$ mixtures as being analogous to the phase separation of polymers in a poor solvent. Thus, the overall manifestation of the interactions is that water functions as a good solvent for the micelles at low temperatures and becomes a poor solvent at high temperatures.

*(b) Microstructural Changes from Linear to Branched Micelles.* An interpretation of the observed cloud points in terms of attractive interactions ignores the dramatic microstructural changes occurring as a function of composition and temperature that are indicated by rheological measurements. The viscosity of EHAC as a function of salt (NaTos or NaSal) shows two maxima, one at low and the other at high salt concentrations (Figures 4 and 7). Because of the intervening two-phase region, there is a break in the curve that obscures the viscosity minimum. Other mixtures of a cationic surfactant and a binding salt, e.g., CTAB/NaSal[3] or CPyCl/NaSal,[2] show a continuous curve with similar viscosity maxima flanking a viscosity minimum. Thus the data are analogous, barring the phase separation at intermediate salt in the present case. (The peak viscosities are also much higher for the samples studied here.)

Phase separation does occur at intermediate salt concentrations in some other micellar systems.[1,28,29] For 4-pentyl and 4-propyl sodium benzoates with CPyCl,[1] the plots of viscosity as a function of salt concentration are strikingly similar to Figure 7a (no temperature dependence of the phase behavior is reported). In contrast, 4-ethyl and 4-methyl sodium benzoates with CPyCl do not show a two-phase region, and in the latter case, there is only a single viscosity maximum.[1] Mixtures of CTAB with low concentrations of the strong hydrotrope sodium 3-hydroxynaphthalene-2-carboxylate (SHNC) also separate into two phases, one of which has a lamellar morphology.[28,29]

These results suggest that highly hydrophobic counterions that can bind strongly to micelles are prone to cause phase separation even at low concentrations. In general, pronounced hydrophobicity in the salt and/or the surfactant is necessary for strong binding. In the above examples, the salt is especially hydrophobic, whereas in the present study, it is the surfactant that is unusually hydrophobic because of its long ($C_{22}$) unsaturated alkyl chains. An analogy can thereby be drawn between phase separation occurring in CPyCl/4-pentyl sodium benzoate and EHAC/NaSal, whereas pairs of relatively less hydrophobic surfactant and salt such as CPyCl/NaSal remain a single phase over the range of compositions.

The link between the rheology and the phase transitions can be further rationalized if they are *both being driven*

(20) Leng, C. A. In *Physics of Amphiphiles: Micelles, Vesicles, and Microemulsions*; Degiorgio, V., Corti, M., Eds.; North-Holland Publishers: Amsterdam, 1983; p 469.
(21) Olsson, U.; Soderman, O.; Guering, P. *J. Phys. Chem.* **1986**, *90*, 5223.
(22) Ulmius, J.; Lindman, B.; Lindblom, G.; Drakenberg, T. *J. Colloid Interface Sci.* **1978**, *65*, 88.
(23) Cassidy, M. A.; Warr, G. G. *J. Phys. Chem.* **1996**, *100*, 3237.
(24) Yu, Z.-J.; Xu, G. *J. Phys. Chem.* **1989**, *93*, 7441.
(25) Mehreteab, A.; Loprest, F. J. *J. Colloid Interface Sci.* **1988**, *125*, 602.
(26) Nakama, Y.; Harusawa, F.; Murotani, I. *J. Am. Oil Chem. Soc.* **1990**, *67*, 717.
(27) Kumar, S.; Sharma, D.; Kabir-ud-Din. *Langmuir* **2000**, *16*, 6821.
(28) Mishra, B. K.; Samant, S. D.; Pradhan, P.; Mishra, S. B.; Manohar, C. *Langmuir* **1993**, *9*, 894.
(29) Horbaschek, K.; Hoffmann, H.; Thunig, C. *J. Colloid Interface Sci.* **1998**, *206*, 439.

*by the same microstructural changes*. Specifically, the first viscosity maximum might signify a shift from linear to branched micelles,[15,30] as a connected network of branched micelles will have a lower viscosity than an entangled network of linear micelles.[30] Recent theories suggest that, as branching proceeds, the system might eventually phase separate into a saturated micellar network (i.e., a branched network with no free ends) and a dilute surfactant solution.[31−33] The driving force for phase separation is the entropic attraction between network junctions.[31]

Micellar branching can thus provide an attractive explanation for the behavior of mixtures such as EHAC/NaSal. Consider first the scenario at ambient temperature. Adding NaSal to EHAC solutions initially causes linear growth of micelles (and an increase in viscosity), followed by micellar branching at higher salt contents (and a decrease in viscosity). The branching proceeds until all the free ends are connected and a saturated network forms. At this point, the system separates into two phases. Incidentally, surfactant packing arguments suggest that a strongly binding salt such as NaSal, which incorporates into the micellar body, can promote the branching of micelles.[15,34]

In light of recent cryo-TEM studies,[35] the branching hypothesis can also explain why EHAC/NaSal samples phase separate on heating. Cryo-TEM observations of the nonionic surfactant pentaethylene glycol monododecyl ether ($C_{12}E_5$) show branched micellar networks in aqueous solutions heated to a cloud point.[35] The reported end-cap energy $E_c$ of $C_{12}E_5$ micelles is particularly high (ca. $54k_BT$ at 25 °C), and $E_c$ was found to increase linearly with temperature. Branching is then predicted to occur when the energy cost to form branches is less than that for end caps, which is a scenario that would become more probable at higher temperatures. Previously,[13] the value of $E_c$ for EHAC/NaSal micelles was estimated as ca. $65k_BT$, with $E_c$ taken to be independent of temperature. This value of $E_c$ is even higher than that for $C_{12}E_5$ and would support a tendency for micellar branching in EHAC/salt samples.

Branched micelles are thus postulated to be the characteristic microstructure in a number of cloud-point systems,[35,36] with phase separation a natural outcome when networks are saturated. Variation of a parameter that promotes branching (such as salt concentration or temperature) can potentially cause phase separation as well. Moreover, as branching proceeds, the viscosity drops, and the tendency for phase separation increases. This explains why the plots of rheological properties and phase transition temperature mirror each other (Figure 4a and b). The lack of phase separation in other cationic systems (such as CTAB/NaSal) could result because a saturated network (with no free ends) is not achieved in those cases. The above microstructural hypothesis, although somewhat speculative, promises to tie together a number of findings from the literature for both nonionic and ionic systems, including the lower consolute phase behavior and the complex trends in rheological properties.

## Conclusions

Mixtures of a $C_{22}$ cationic surfactant and a salt with a hydrophobic counterion often show lower consolute phase behavior. The microstructure in these solutions consists of wormlike micelles, and the rheology shows a complex variation as a function of salt. On heating to the cloud point, the viscosity decreases, whereas the intensity of scattered light and neutrons increases. The data are consistent with theories of critical phenomena. A plausible hypothesis is that the binding of hydrophobic counterions promotes micellar branching. As free micellar ends are incorporated into a branched network, the viscosity drops, and the entropic attraction between junctions eventually causes phase separation. Branched micelles might also develop on heating the solution, in analogy with observations of some nonionic micellar systems. The similarity between viscosity and cloud-point data is also consistent with the branching mechanism.

**Acknowledgment.** We acknowledge the National Institute of Standards and Technology, U.S. Department of Commerce, in facilitating the SANS experiments performed as part of this work. H.E. gratefully acknowledges the Swedish Foundation for International Cooperation in Research and Higher Education, STINT, for a postdoctoral fellowship.

LA011148E

(30) Lequeux, F. *Europhys. Lett.* **1992**, *19*, 675.
(31) Drye, T. J.; Cates, M. E. *J. Chem. Phys.* **1992**, *96*, 1367.
(32) Panizza, P.; Cristobal, G.; Curely, J. *J. Phys. Condens. Matter* **1998**, *10*, 11659.
(33) Cristobal, G.; Rouch, J.; Curely, J.; Panizza, P. *Physica A* **1999**, *268*, 50.
(34) Lin, Z. *Langmuir* **1996**, *12*, 1729.
(35) Bernheim-Groswasser, A.; Wachtel, E.; Talmon, Y. *Langmuir* **2000**, *16*, 4131.
(36) Bernheim-Groswasser, A.; Tlusty, T.; Safran, S. A.; Talmon, Y. *Langmuir* **1999**, *15*, 5448.